THE DEACTIVATION OF VIBRATIONALLY EXCITED CARBON DIOXIDE (001) BY COLLISIONS WITH CARBON MONOXIDE

W.A. Rosser, Jr., R.D. Sharma and E.T. Gerry

RESEARCH REPORT 349
Contract No. F29601-69-C-0060
Project: 3326
September 1970

prepared for

AIR FORCE WEAPONS LABORATORY
AIR FORCE SYSTEMS COMMAND
UNITED STATES AIR FORCE
Kirtland Air Force Base, New Mexico

and

ADVANCED RESEARCH PROJECTS AGENCY
ARPA Order No. 870

AVCO EVERETT RESEARCH LABORATORY
A DIVISION OF AVCO CORPORATION

DISCLAIMER NOTICE

THIS DOCUMENT IS THE BEST QUALITY AVAILABLE.

COPY FURNISHED CONTAINED A SIGNIFICANT NUMBER OF PAGES WHICH DO NOT REPRODUCE LEGIBLY.

THE DEACTIVATION OF VIBRATIONALLY EXCITED CARBON DIOXIDE (001) BY COLLISIONS WITH CARBON MONOXIDE

by

W. A. Rosser, Jr., R. D. Sharma and E. T. Gerry

AVCO EVERETT RESEARCH LABORATORY
a division of
AVCO CORPORATION
Everett, Massachusetts

Contract No. F29601-69-C-0060
Project: 3326

September 1970

prepared for

AIR FORCE WEAPONS LABORATORY
AIR FORCE SYSTEMS COMMAND
UNITED STATES AIR FORCE
Kirtland Air Force Base, New Mexico

and

ADVANCED RESEARCH PROJECTS AGENCY
ARPA Order No. 870

ABSTRACT

The rate constants associated with the deactivation of vibrationally excited CO_2^* (001) by collisions with CO have been experimentally determined from 300 to 900°K by a laser fluorescence method. These reactions involving CO considered were:

$$CO_2^* (001) + CO \underset{k_2}{\overset{k_1}{\rightleftharpoons}} CO_2 + CO^* (v = 1)$$

$$CO_2^* (001) + CO \xrightarrow{k_{CO}} CO_2 + CO$$

$$CO^* (v = 1) + CO_2 \xrightarrow{k_4} CO + CO_2.$$

Within experimental error the rate constant k_1 increases linearly with temperature T (°K) from a value of 5.7×10^3 $torr^{-1} sec^{-1}$ at room temperature to a value of 11.2×10^3 $torr^{-1}$ sec^{-1} at 900°K. From 500 to 900°K the rate constant k_{CO} ($torr^{-1}$ sec^{-1}) varies with temperature as

$$\log_{10} k_{CO} = A - BT^{-1/3}$$

with A = 6.61 and B = 31.6. From 300 to 500°K the measured values of k_{CO} are greater than those corresponding to the cited relation. The rate constant k_4 was found to be negligible compared to k_{CO}.

The probability per collision of vibrational energy transfer from CO_2^* (001) to CO (v = 0) was computed by a theory involving long range forces. The calculated probabilities are in good agreement with the probabilities deduced from measurement of R_1, the transfer rate constant in the exothermic direction.

TABLE OF CONTENTS

		Pag
	Abstract	iii
I.	INTRODUCTION	1
II.	EXPERIMENTAL	5
	A. Apparatus	5
	B. Analysis of Experimental Records	8
	C. Data Analysis	11
	D. Theoretical	24
	REFERENCES	37

I. INTRODUCTION

A CO_2 laser provides an excellent means of studying the collisional deexcitation of CO_2^* (001). A pulse of 10.6μ radiation from a Q-switched CO_2 laser may be used to produce in a test gas containing CO_2 a nonequilibrium population of CO_2^* (001).[1-3] The return to equilibrium may be studied by monitoring the fluorescence radiation in the vicinity of 4.3μ. The method is adaptable to study in a temperature range (300 to $\approx$ 1000°K) not easily attainable by shock tube methods but readily attainable by conventional electric heating. A wide attainable temperature range is desirable in order to establish with precision the small temperature coefficients associated with the collisional deexcitation of CO_2^*.

In the absence of vibration-vibration coupling, the fluorescense signal S decays exponentially with time following excitation by a laser pulse, $S = S_o e^{-Rt}$, and the decay constant R, a function of temperature, pressure, and gas composition, may be determined from the linear variation of log S with time. The decay constant R when normalized to unit pressure is a weighted average of the specific rate constants associated with the processes

$$CO_2^* (001) + M \xrightarrow{k_M} CO_2 + M \qquad (1)$$

$$CO_2^* (001) + CO_2 \xrightarrow{k_C} CO_2 + M \qquad (2)$$

where M is any substance other than CO_2 present in the system. Given a knowledge of k_C,[1] a value for k_M, the desired quantity, can be extracted from $\bar{k} = R/p$, p being the total gas pressure.

In the kinetically more complicated case of a substance M with a vibrational level that couples to that of CO_2^* (001), one must include in the reaction mechanism the pair of coupling reactions

$$CO_2^*(001) + M \underset{k_M''}{\overset{k_M'}{\rightleftarrows}} CO_2 + M^* \qquad (3)$$

as well as an additional pair of degradation reactions

$$M^* + CO_2 \xrightarrow{k_{4a}} M + CO_2 \qquad (4a)$$

$$M^* + M \xrightarrow{k_{4b}} M + M. \qquad (4b)$$

In such cases the signal S will vary with time as the sum of two exponentials, $S = S_1 e^{-\lambda_1 t} + S_2 e^{-\lambda_2 t}$, where both λ_1 and λ_2 depend on the rates of all the significant reactions.[1] Under favorable circumstances one can deduce from measurement of λ_1, λ_2, and the ratio S_1/S_2, values for the pertinent rate constants. Such was the case in earlier study of the system CO_2/N_2 which led to determination of k_C, $k_M(N_2)$, $k_M'(N_2)$, and $k_M''(N_2)$ in the temperature range from 300 to 1000°K. The present study of the CO_2/CO system was carried out to obtain similar information for M = CO. The two systems CO_2/N_2 and CO_2/CO differ in that Eq. (3) for M = N_2 is almost thermoneutral whereas for M = CO, the energy mismatch is about 200 cm^{-1}. The kinetic consequences for k_M' and k_M'' of this mismatch were of particular interest.

In a previous study the vibration-to-vibration (V-V) energy transfer (Eq. 3) for CO_2-N_2 was explained by long range forces using dipole-quadrupole coupling.[4] The dipole moment matrix element between 000 and 001 states of CO_2 interacts with the quadrupole matrix element between vibrational states of N_2 having 0 and 1 quantum of vibrational excitation leading to energy transfer. Since then the theory has been applied to a number of situations[5-7] and has yielded results in satisfactory agreement with experiment. The results are accurate to $\sim$ 25% if the first order theory is applicable and seems to be within a factor of 2 if the second order theory is used. The present situation affords an opportunity to apply the theory to a case where the energy mismatch is greater than in any of the cases already considered.

The experimental values for the square of the matrix element of the dipole moment[8] for the first fundamental as well as for the permanent[9] quadrupole moment are available. Calculations for the variation of the quadrupole moment[10,11] and octupole moment[11] with internuclear distance have been performed. The molecular parameters needed are thus available from independent sources and a comparison of the calculated results with the experimental values of the V-V transfer rate is expected to put the theory to a comprehensive test.

II. EXPERIMENTAL

A. Apparatus

The experimental apparatus, shown schematically in Fig. 1, has been described elsewhere.[1] Consequently, the present description will be less detailed. Laser operating conditions were chosen to optimize the fluorescence signals. These conditions were a laser pressure of about 17 torr and a regulated discharge current of 30 ma (12 to 13 kV) with a premixed laser mixture consisting of 11% CO_2, 8% N_2, and 81% He. At the usual switching rate of 300 cps a laser pulse consisted of two closely spaced pulses with an overall length of about 1 1/2 μsec.

The reaction cell consisted in essence of a 1" o.d. stainless steel tube with provision for heating the center section of the cell. The furnace, a resistance wire type conventional in design except for the adaptation to a cell of awkward shape, included a heavy-walled nickel shell to insure uniformity of heating. Cell temperature was measured by means of four 24-gauge chromel-alumel thermocouples in contact with the center portion of the cell wall. The cell and furnace assembly is useable up to about 1000°K.

The windows (C) required to transmit the fluorescence radiation were of sapphire (3/4 inch diameter) brazed with silver to a Kovar sleeve (Ceramics International Corp.) which was itself welded to the cell body. Light emerging from the cell was transmitted to the detector by means of a 6 inch Vycor light pipe internally plated with platinum. At cell

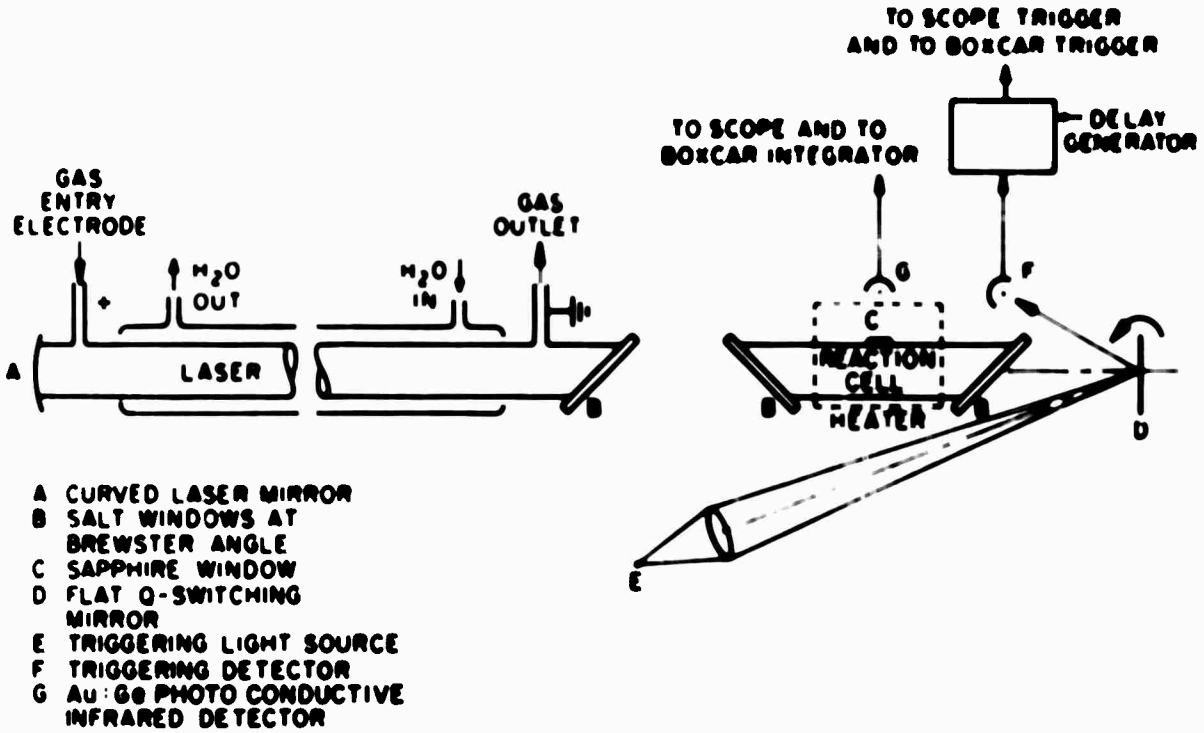

Fig. 1 Schematic diagram of fluorescence apparatus.

temperatures greater than about 700°K, it was necessary to cap the pipe with a small Irtran 2 lens (1 inch diameter, 1 inch focal length) in order to prevent excessive heating of the detector and holder.

The detection system included: (1) a Au:Ge photoconductive detector used in a conventional manner; (2) a Keithly 102B amplifier (1000 gain, 2 cps to either 150 kc or 1.7 Mc); (3) a Tektronix Model 535 oscilloscope for visual monitoring of the amplified fluorescence signal; (4) a Box-Car Integrator (Princeton Applied Research, Model CW-1) and an associated X-Y Recorder. An integration device is necessary because of the very unfavorable ratio of signal to noise of single traces at elevated cell temperatures. Integration times varied from 5 to 20 minutes.

The gas-handling system associated with the reaction cell included a lecture bottle source of bone-dry CO_2 (J. T. Baker, > 99.8% pure) and a similar source of research grade CO (Matheson Co.). Mixing of CO and CO_2 in a storage vessel was accomplished by overnight diffusion. Gas samples were admitted as needed to a small pyrex manifold with attachments to the reaction vessel, to a Manostat manometer (0 - 1 atm) and to a Dubrovin gauge (0 - 20 torr).

Measurements were usually carried out in the following way. A gas sample was admitted to the reaction cell and one or two X-Y records of the box car signal obtained. Usually, the mixture was then discarded and another sample admitted to the cell. The process was repeated until a satisfactory set of records had been obtained. Periodically, the temperature of the four thermocouples in contact with the cell wall were measured. The

arithmetical average of the measured temperatures was considered to be the reaction temperature. The spread in temperature among the four thermocouples was insignificant!

B. Analysis of Experimental Records

Relaxation of excess vibrational energy in a mixture of CO_2 and CO involves both V-V coupling between CO_2 and CO and T-V degradation with the consequence that the observed signal S is expressible as the sum of two exponential terms.

$$S = S_1 e^{-\lambda_1 t} + S_2 e^{-\lambda_2 t} \quad (\lambda_1 > \lambda_2) \tag{5}$$

The kinetic significance of the measurable quantities λ_1, λ_2, and S_1/S_2 is discussed in the following section. This section is devoted primarily to a description of the manner in which the desired data were obtained.

By proper choice of the mixture ratio ψ_C/ψ_{CO}, where ψ_C and ψ_{CO} are the mole fractions of CO_2 and CO respectively, the decay constant λ_1 can be made much greater than λ_2. In this study, ratios of $\psi_C/_{CO} = 1$, 1/2, and 1/4 were used. As a consequence of the difference between λ_1 and λ_2, the overall reaction can be partitioned into two distinct but overlapping time periods, an early time period during which Eq. 5 is dominated by the term $S_1 e^{-\lambda_1 t}$ and a late time period dominated by the term $S_2 e^{-\lambda_2 t}$. The situation is illustrated in Fig. 2.

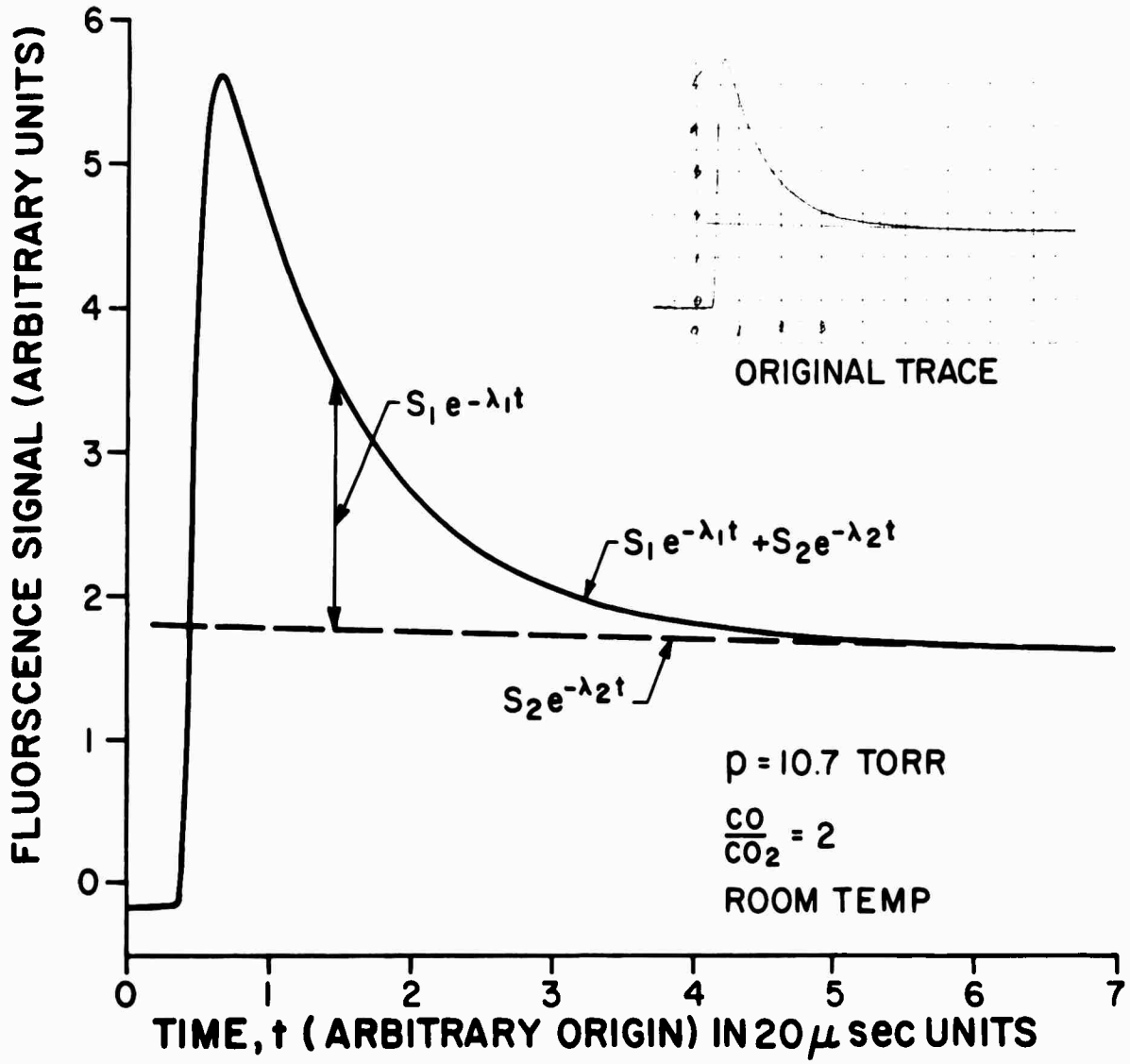

Fig. 2 Schematic of fluorescence record for CO_2/CO mixture.

Since, for sufficiently late times the signal S is nearly equal to $S_2 e^{-\lambda_2 t}$, the decay constant λ_2 can be determined from the late time fluorescence trace. The usual pressure range used in obtaining clearly defined late time histories was 20 to 200 torr. The initial time portion of a trace during which $S_1 e^{-\lambda_1 t}$ contributes to the signal was ignored and was in most cases useless because of distortion resulting from the inability of the measurement system to respond to the very high rate of change during the early time period. Determination of λ_2 from a late time history was sometimes complicated by slight base line shifts (a few percent of peak height in the direction of increasing signal) that appeared at high reaction temperatures ($T > 600^{\circ}K$). These base line shifts have been attributed to a sligh degree of gas heating associated with the absorption and degradation of laser energy and are discussed elsewhere.[1] In such cases the signal S was referred to the final base line. Then λ_2 was determined in the usual manner from the slope of the linear variation of $\log_{10} S$ with time. The normalized data $\lambda_2^{\,1} = \lambda_2/p$, where p is total pressure, are shown in Fig. 3 for values of $\psi_C/\psi_{CO} = 1,\ 1/2$, and $1/4$ and temperatures in the range from 300 to $1000^{\circ}K$. The precision of measurement decreased from a few percent at room temperature to about $\pm$ 10% at high temperatures ($T \gtrsim 700^{\circ}K$), primarily because of a pronounced decrease in the ratio of signal to noise at high temperature.

Once $\lambda_2^{\,1}$ has been determined, additional measurements can be made over the desired temperature range but at pressures such that the early time history is clearly defined. Analysis of the quantity $S_1 e^{-\lambda_1 t}$, a positive quantity at pressures suitable for a determination of λ_1, during

this early time period leads to the decay constant λ_1 and a value of S_1 if desired. However, since the measured signal is S, the quantity $S_2 e^{-\lambda_2 t}$ must be calculated and subtracted from S. To accomplish this, $\lambda_2 = \lambda_2{}^1 p$ is first calculated with the aid of Fig. 3 for the experimental values of temperature and pressure. Then, using a value of S, relative to a shifted base line at high temperature, selected from the trace at a time t such that $S \approx S_2 e^{-\lambda_2 t}$, the value of S_2 is found. Considering now the measured values of S in the early time period, together with the calculated values of S_2 and λ_2, the time dependence of the function $S_1 e^{-\lambda_1 t}$ is found. Again plotting the log of this function versus t leads to a value of λ_1, and the intercept of the resulting straight line with the $t = 0$ axis determines S_1.

In general, λ_1 was determined over a range of 5 to 20 torr and the results averaged and normalized graphically at low temperatures and arithmetically at high temperatures. The normalized data, $\lambda_1{}^1 = \lambda_1/p$ are presented in Fig. 4. Precision of measurement varied from a few percent to $\pm$ 10% depending on reaction temperature and mixture composition. Values of S_1/S_2 were determined for $\psi_C/\psi_C = 1/4$ using a small absorption cell filled with CO placed between the exit of the light pipe and the detector in order to reduce the contribution of CO^* radiation to the observed signal. These data, of limited accuracy because of the long extrapolation of the signal to the time origin, are shown in Table II along with numerical results discussed in the following section.

C. Data Analysis

When a mixture of CO_2 and CO is exposed to a laser pulse, absorption of a portion of the pulse energy by CO_2 molecules in the lower

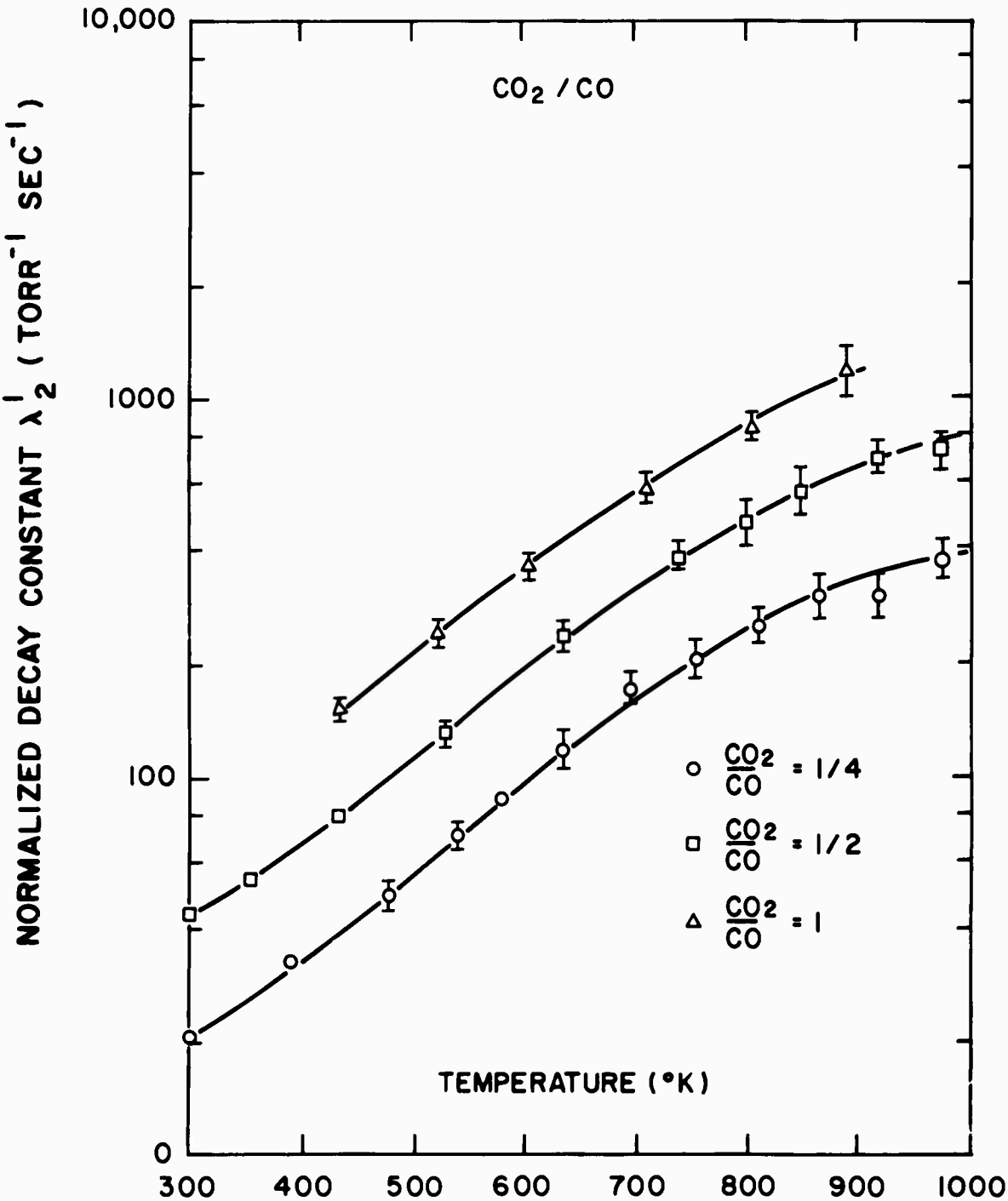

Fig. 3 CO_2/CO: The normalized decay constant λ'_2 as a function of temperature.

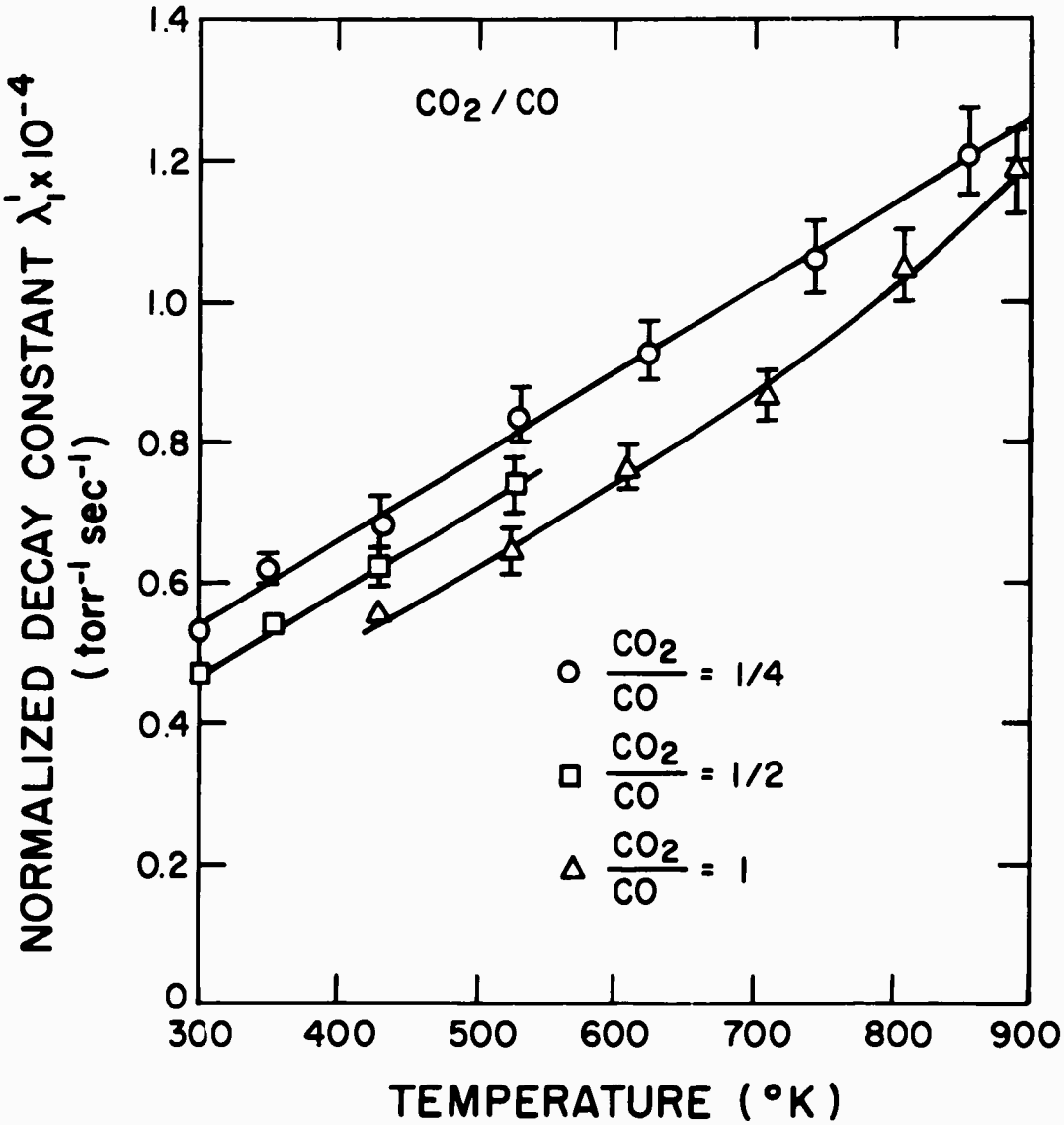

Fig. 4 CO_2/CO: The normalized decay constant λ_1' as a function of temperature.

laser level (100) creates a nonequilibrium population of CO_2 molecules in the upper laser level (001). At low reaction temperatures it may be assumed that the excess vibrational energy is not redistributed to a significant degree throughout the other levels of the ν_3 mode. Similarly, it may be assumed that vibrational energy transferred from CO_2^* (001) to CO is localized in the level CO^* (v = 1). For present purposes, therefore, attention has been limited to these reactions:

$$CO_2^* (001) + CO \underset{k_2}{\overset{k_1}{\rightleftharpoons}} CO_2 + CO^* (v = 1) + 206\ cm^{-1} \qquad (6)$$

$$CO_2^* (001) + M\ (M = CO_2,\ CO) \xrightarrow{\overline{k}_3} CO_2 + M \qquad (7)$$

$$CO^* (v = 1) + M\ (M = CO_2,\ CO) \xrightarrow{\overline{k}_4} CO + M \qquad (8)$$

The reaction scheme involves four rate constants. Of these, k_1 and k_2 are related to each other and to the temperature T (^oK) by Eq. (9)

$$\frac{k_2}{k_1} = K = e^{-295/T} \qquad (9)$$

The rate constants $\overline{k}_3$ and $\overline{k}_4$, measures of the net rate of energy degradation, are weighted averages for M = CO_2 and CO and therefore vary in general with mixture composition as well as with temperature.

Corresponding to the reaction mechanism are these two coupled linear first order differential equations in the dependent variables $X = (CO_2^* - \overline{CO_2})$ and $y = (CO^* - \overline{CO})$ where $\overline{CO}_2$ and $\overline{CO}$ are respectively the equilibrium populations of CO_2^* (001) and CO^* (v = 1).

AVCO EVERETT RESEARCH LABORATORY
a Division of
AVCO CORPORATION
Everett, Massachusetts

Contract No.
Project No.

September 1970

prepared for

AIR FORCE WEAPONS LABORATORY
AIR FORCE SYSTEMS COMMAND
UNITED STATES AIR FORCE
Kirtland Air Force Base, New Mexico

and

ADVANCED RESEARCH PROJECTS AGENCY
ARPA Order No. 870

$$\frac{dx}{dt} = (-k_1 p_{CO} - \overline{k}_3 p_M)\, x + k_1 p_C K\, y \tag{10}$$

$$\frac{dy}{dt} = k_1 p_{CO}\, x + y\,(-k_1 p_C K - \overline{k}_4 p_M) \tag{11}$$

It is known[12] that both x and y vary with time as

$$x = A_1 e^{-\lambda_1 t} + B_1 e^{-\lambda_2 t} \tag{12}$$

$$y = A_2 e^{-\lambda_1 t} + B_2 e^{-\lambda_2 t} \tag{13}$$

with decay constants λ_1 and λ_2 given by

$$2\lambda_{1,2} = R_1 \pm \sqrt{R_1^2 - 4R_2} \quad (\lambda_1 > \lambda_2) \tag{14}$$

where

$$R_1 = k_1 p_{CO} + k_1 p_C K + \overline{k}_3 p_M + \overline{k}_4 p_M \tag{15}$$

$$R_2 = k_1 \overline{k}_4 p_{CO} p_M + \overline{k}_3 \overline{k}_4 p_M^2 + k_1 \overline{k}_3 p_C p_M K \tag{16}$$

or in normalized form $\lambda_1^{\,1} = \lambda_1 / p_M$, $\lambda_2^{\,1} = \lambda_2 / p_M$

$$R_1^{\,1} = k_1 \psi_{CO} + k_1 \psi_C K + \overline{k}_3 + \overline{k}_4 \tag{17}$$

$$R_2^{\,1} = k_1 \overline{k}_4 \psi_{CO} + \overline{k}_3 \overline{k}_4 + k_1 \overline{k}_3 \psi_C K \tag{18}$$

with ψ_{CO} and ψ_C equal respectively to the mole fractions of CO and CO_2. It may be shown from the initial conditions that

$$\frac{A_1}{B_1} = \frac{\lambda_2^{1} \cdot k_1 \nu_{CO} \cdot \bar{k}_3}{\lambda_1 \cdot k_1 \nu_{CO} \cdot \bar{k}_3} \qquad (19)$$

If fluorescence radiation from CO^* does not contribute significantly to the observed signal S, then the ratio A_1/B_1 may be identified with the measurable quantity S_1/S_2. In that case, Eqs. (17), (18), and (19) constitute a system of three equations in the three unknowns k_1, $\bar{k}_3$, $\bar{k}_4$ and measurement of λ_1^{1}, λ_2^{1}, and S_1/S_2 provides sufficient information to establish values for k_1, $\bar{k}_3$, and $\bar{k}_4$. This was the case in an earlier and similar study[1] of the CO_2–N_2 system. Because N_2^* ($v = 1$) does not radiate, the observed signal was due to CO_2^* alone and the ratio S_1/S_2 was measured with sufficient accuracy to demonstrate that $k_4(N_2)$ could be ignored relative to $\bar{k}_3$. In the present case, both CO^* and CO_2^* can contribute to the signal and unless radiation from CO^* is suppressed, a value of S_1/S_2 is an unreliable measure of the ratio A_1/B_1. Measurement of λ_1 and λ_2 alone is then insufficient to determine k_1, $\bar{k}_3$, and $\bar{k}_4$.

Fortunately, the relative importance of $\bar{k}_3$ and $\bar{k}_4$ can be established using the λ_2 data of Fig. 3. A noteworthy feature of that data is that at a given temperature, λ_2^{1} is closely proportional to the ratio ν_C/ν_{CO}. It can be shown that the observed proportionality is consistent with $\bar{k}_3 \gg \bar{k}_4$ but inconsistent with the converse $\bar{k}_4 \gg \bar{k}_3$. Consider Eq. (14). Typically, in this study $R_2/R_1^2 < 0.1$. Consequently, the square root term can be approximated by a two term expansion with the result that

$$\lambda_2^{\,1} = \frac{R_2^{\,1}}{R_1^{\,T}} \quad \frac{k_1 \bar{k}_3 \nu_C K \left(1 + \frac{\bar{k}_4}{k_1 \nu_C K} + \frac{\bar{k}_4 \psi_{CO}}{\bar{k}_3 \psi_C K}\right)}{k_1 \nu_{CO}\left(1 + \frac{\nu_C K}{\nu_{CO}}\right) + \bar{k}_3\left(1 + \frac{\bar{k}_4}{\bar{k}_3}\right)} \tag{20}$$

For $\bar{k}_4 = 0$, Eq. (20) becomes

$$\frac{R_2^{\,1}}{R_1^{\,T}} = \frac{k_1 \bar{k}_3 \nu_C K}{k_1 \psi_{CO}\left(1 + \frac{\psi_C K}{\psi_{CO}}\right) + \bar{k}_3} \tag{21}$$

If, in addition, $\bar{k}_3 = k_1$, as is probably true, then Eq. (21) reduces to Eq. (22)

$$\frac{R_2^{\,1}}{R_1^{\,T}} = \frac{\bar{k}_3 K}{\left(1 + \frac{\psi_C K}{\psi_{CO}}\right)} \quad \frac{\psi_C}{\psi_{CO}} \tag{22}$$

or, with rearrangement and substitution of the relation $\bar{k}_3 = k_C \psi_{CO_2} + k_{CO} \psi_{CO}$, to Eq. (23)

$$\lambda_2^{\,1}\left(1 + \frac{\nu_C K}{\psi_{CO}}\right) = K \psi_C k_{CO}\left(1 + \frac{k_C \psi_C}{k_{CO} \psi_{CO}}\right) \tag{23}$$

In a similar manner it can be shown that the assumption $\bar{k}_3 = 0$ leads to Eq. (24)

$$\lambda_2^{\,1}\left(1 + \frac{\psi_C K}{\psi_{CO}}\right) = \bar{k}_4 \tag{24}$$

Of the two components of k_4, that corresponding to the reaction

$$CO^* + CO \rightarrow CO + CO \tag{25}$$

is known to be negligibly small.[13] Consequently, $\bar{k}_4 \quad k_{4C}\psi_C$ where k_{4C} refers to the process

$$CO^* + CO_2 \xrightarrow{k_{4C}} CO + CO_2 \tag{26}$$

In terms of k_{4C}, Eq. (24) becomes

$$\lambda_2^1 \left(1 + \frac{\psi_C K}{\psi_{CO}}\right) \quad k_{4C}\psi_C \tag{27}$$

According to Eq. (23) the quantity $\lambda_2^1 \left(1 + \frac{\psi_C K}{\psi_{CO}}\right)$ varies nonlinearly with ψ_C to a degree that depends on the ratio k_C/k_{CO} whereas by Eq. (27), $\lambda_2^1 \left(1 + \frac{\psi_C K}{\psi_{CO}}\right)$ is strictly proportional to ψ_C. The different dependence on ψ_C of Eqs. (23) and (27) permits a choice to be made between the case $\bar{k}_3 \cdot \bar{k}_4$ and $\bar{k}_4 \quad \bar{k}_3$, using the data of Fig. 3. As shown in Fig. 5 the variation of $\lambda_2^1 \left(1 + \frac{\psi_C K}{\psi_{CO}}\right)$ with ψ_C is markedly nonlinear, indicating that $\bar{k}_3 \cdot \bar{k}_4$. Further, replotting $\lambda_2^1 \left(1 + \frac{\psi_C}{\psi_{CO}} K\right)$ as a function of $\psi_C \psi_{CO}$ results in a nearly linear relation, indicating that $\bar{k}_3$ is insensitive to mixture ratio, and that k_C and k_{CO} are comparable in magnitude.

With the simplification $\bar{k}_4 \quad 0$ the data shown in Figs. 3 and 4 were analyzed numerically. The results of that analysis are ambiguous in that to a pair of values for $\lambda_{1,2}$ there corresponds two solutions differing markedly in values for k_1, $\bar{k}_3$ and A_1/B_1. The correct solution can be selected either by physical reasoning ($\bar{k}_3 \cdot k_1$ at least at low temperatures)

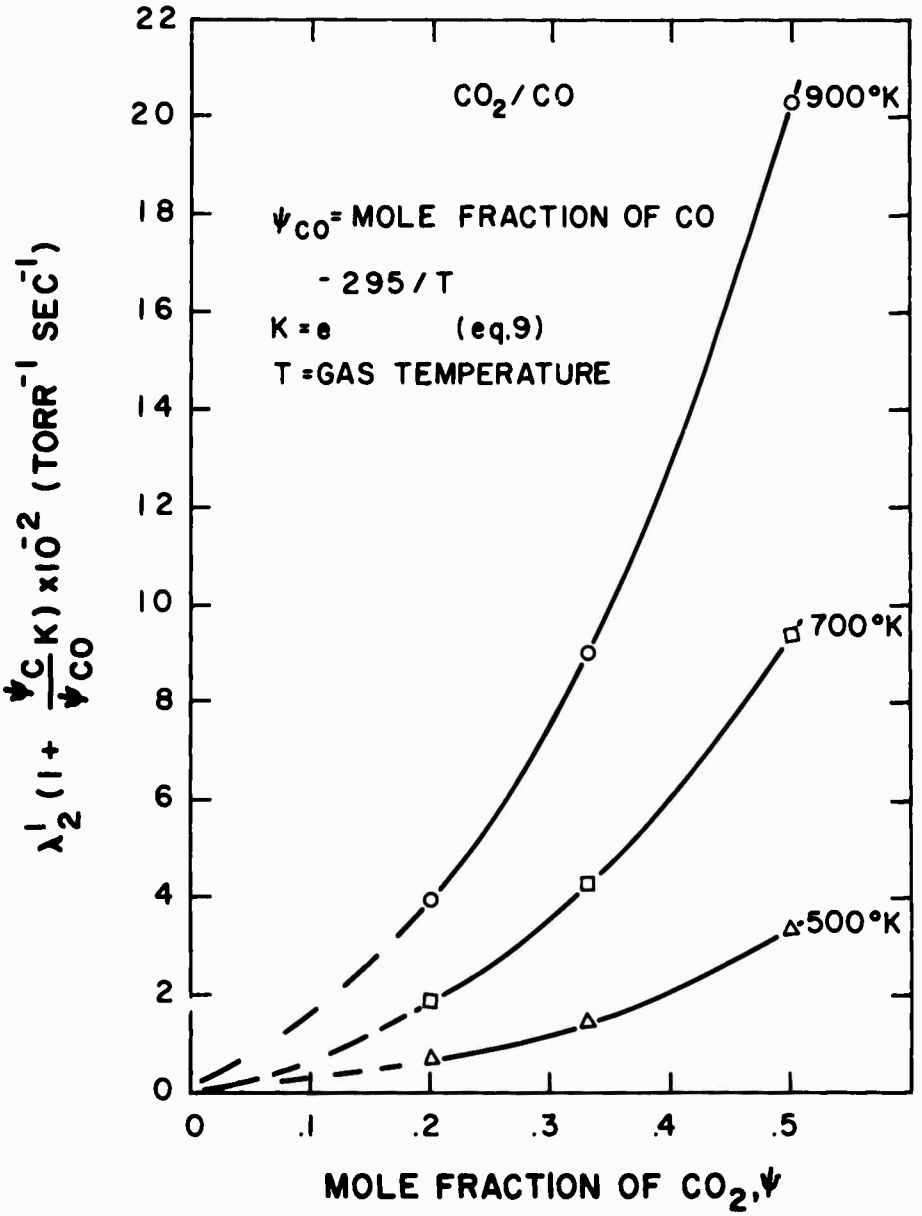

Fig. 5 CO_2/CO: Variation of $\lambda_2'(1+\frac{\psi_C}{\psi_{CO}}k)$ with ψ_C the mole fraction of CO_2.

B5540

or by an approximate measurement of S_1/S_2. Such measurements were available for ψ_C/ψ_{CO} 1.4. (See Table I.) Both approaches lead to the same choice of solutions. The results of the analysis for k_1 are shown graphically in Fig. 6. Within experimental error, k_1 increases linearly with temperature unlike the behavior of the analogous k_1 for CO_2/N_2 shown in Fig. 6 for comparative purposes.

As noted earlier, the degradation rate constant $\bar{k}_3$ is a weighted average of k_C and k_{CO}, $\bar{k}_3 = \psi_C k_C + \psi_{CO} k_{CO}$,

$$CO_2^* + CO_2 \xrightarrow{k_C} CO_2 + CO_2 \tag{28}$$

$$CO_2^* + CO \xrightarrow{k_{CO}} CO_2 + CO . \tag{29}$$

Given a knowledge of k_C,[1] values of k_{CO} were extracted from $\bar{k}_3$ with the results shown graphically in Fig. 7 in conventional Landau-Teller form, $\log_{10} k_{CO}$ as a function of $T^{-1/3}$. At high temperatures ($T > 500^\circ K$), the variation of k_{CO} with temperature can be represented by $\log_{10} k_{CO} = A - BT^{-1/3}$ with A 6.61 and B 31.6. As in the case of k_C[1] and k_{N_2}[1] the nonlinearity at low temperature is attributed to the existence of a shallow well in the potential function describing the interaction of CO_2^* with CO, as suggested by theoretical analysis of the collisional deactivation of vibrationally existed diatomic molecules.[14-16]

TABLE I. Intercept ratio S_1/S_2 as a function of temperature

T (^{o}K)	$\frac{S_1}{S_2}$ (Exp)	$\left(\frac{S_1}{S_2}\right)^{*}$	$\left(\frac{S_1}{S_2}\right)^{\dagger}$
300	10 - 11	11.4	5525
351	10	9.9	4962
434	8 - 9	8.6	3275
536	8	7.8	1947
630	9 - 10	7.8	841
744	7 - 8	8.1	348
858	6 - 7	8.5	213

* Eq. (19), correct solution

† Eq. (19), wrong solution

ψ_C = mole fraction of CO_2

ψ_{CO} = mole fraction of CO

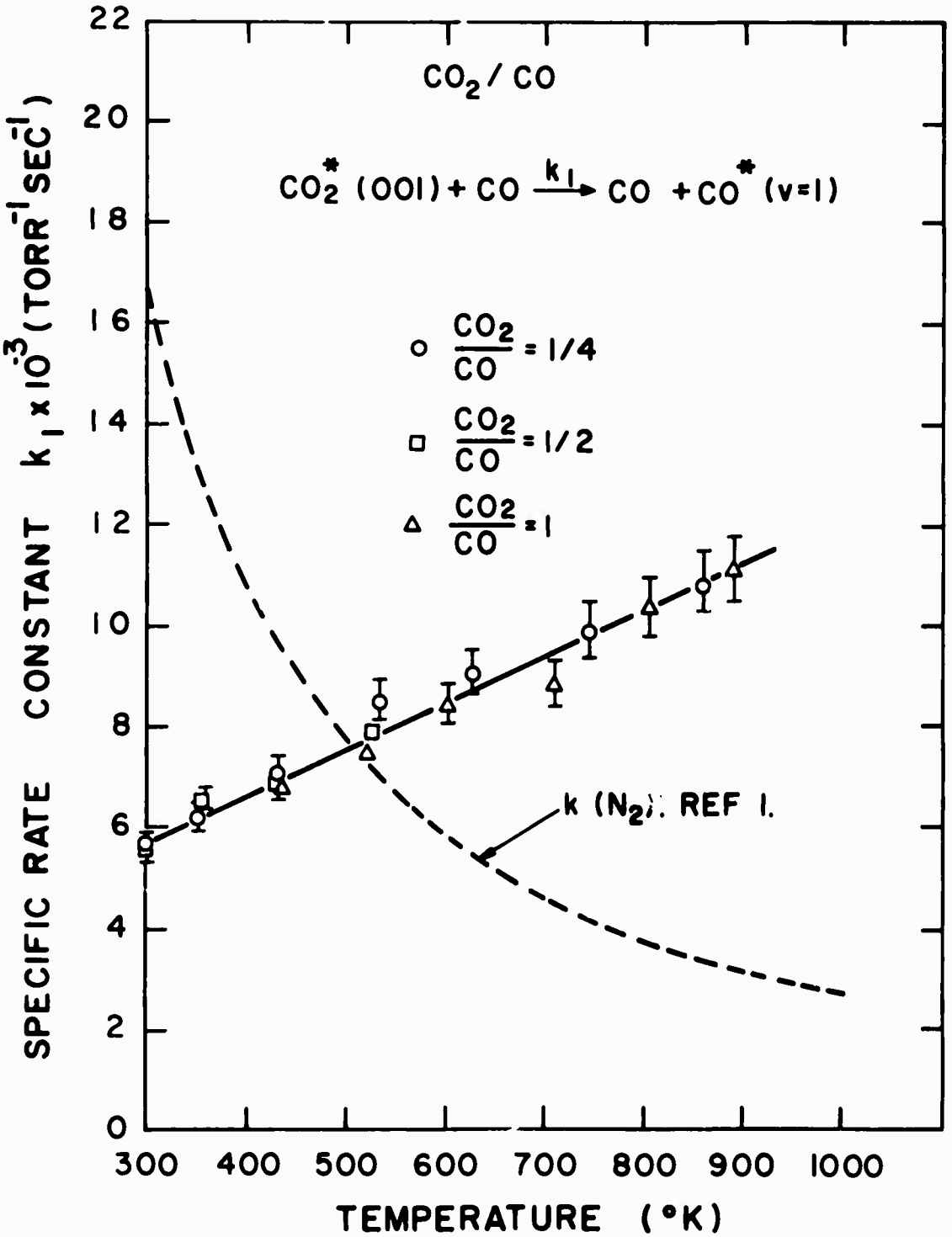

Fig. 7 CO_2 / CO. Variation of the transfer rate constant with temperature.

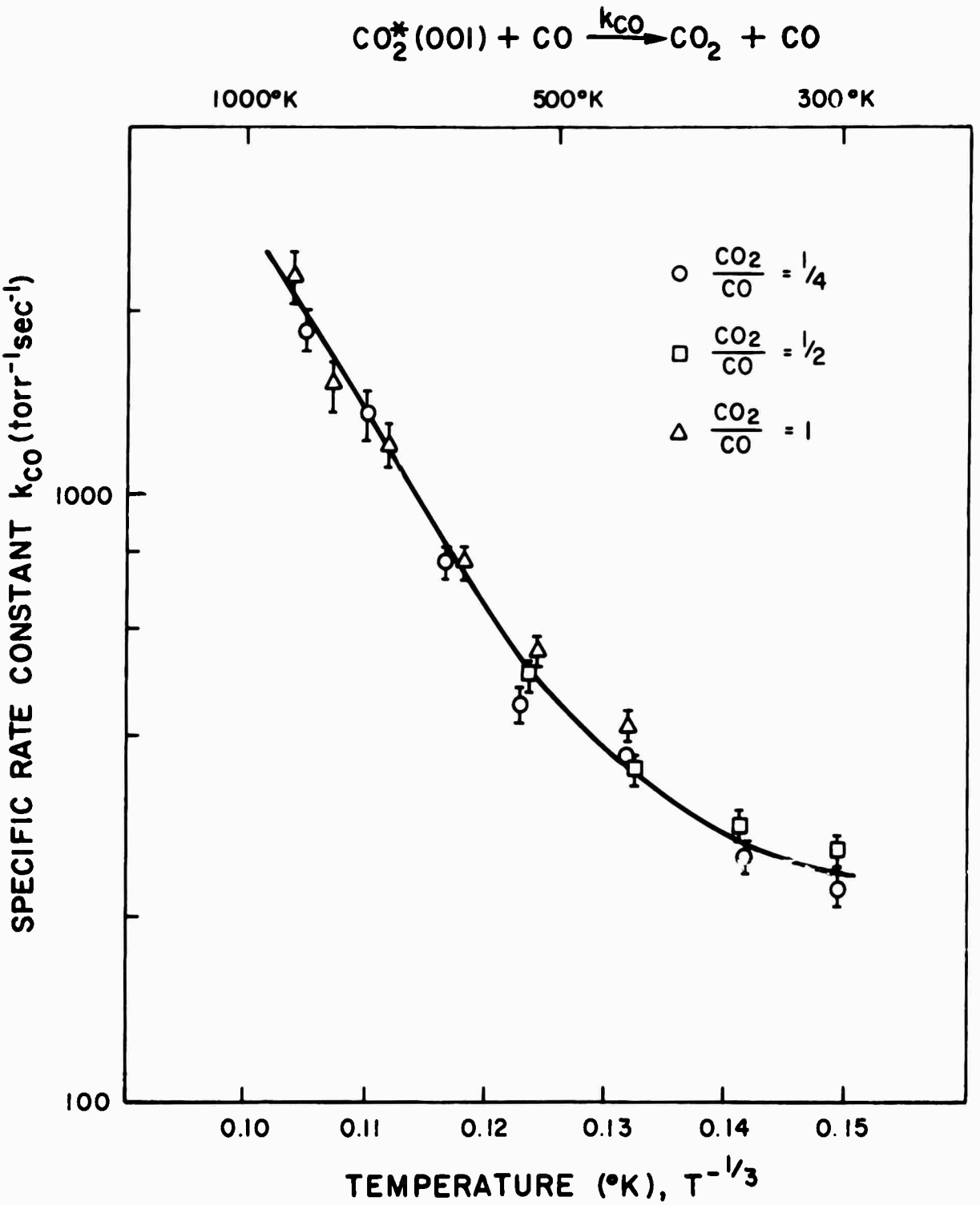

Fig. 7 CO_2/CO: Variation of the degradation rate constant with temperature.

B4417

D. Theoretical

The value of the specific reaction rate for vibration to vibration energy transfer (Fig. 6) corresponds to a probability of energy exchange for collision P equal to 0.5×10^{-4} and 2.1×10^{-3} at 300 and 900°K, respectively. P increases monotonically with temperature and at higher temperatures, where the signal to noise problems are severe, is estimated to have a precision of about $\pm$ 10%. At lower temperatures the experiments are more reliable. Interestingly enough the values of P obtained by a Landau-Teller[17] or Schwartz-Slawsky-Herzfield[18] type calculation are of the magnitude cited above. For example, Rapp[19] calculates P for the reaction.

$$AB\ (v = 1) + CD\ (v = 0) \xrightarrow{P} AB\ (v = 0) + CD\ (v = 1) + 200\ cm^{-1} \qquad (30)$$

in the exothermic direction to be about 8×10^{-4} at 300°K and increasing to about 4×10^{-3} at 1000°K. A claculation of the probabilities V-V energy transfer due to long range forces then affords an opportunity to compare two predictions based on entirely different premises with each other and with the experimental results.

The calculation of the V-V rates due to long range forces is divided into two parts, the contributions to the rate in the first and second order perturbation expansions. The first order calculation was first presented by Sharma and Brau[4] and has proven its usefulness in a variety of situations.[5,6] The second order calculation to be used here has been presented[7] elsewhere. This calculation is valid when $\omega_{vi}\tau > 1$ where ω_{vi} is the energy difference between the virtual and initial state divided by $\hbar$ and τ is the time duration of the collision. The usefulness of this calculation has been demonstrated by applying it to the V-V transfer reaction

$$CO_2(001) + N_2O(000) \rightarrow CO_2(000) + N_2O(001) + 125.8\ cm^{-1} \qquad (31)$$

the rate constant of which has been measured[20] at room temperature. The first order and second order calculations are expected to be accurate to about 25% and a factor of about 2, respectively.

In the first order calculation we will calculate the rate constant due to dipole-dipole interaction alone. We will discuss the contribution of the higher multipoles later in the paper. The reason for doing this is that only the dipole moment matrix elements are known with confidence. There are several calculations[10] for the quadrupole moment and all of these give reasonable agreement with the experimentally measured value.[9] Two of these[10, 11] calculate quadrupole moment as a function of internuclear distance. However, past experience[4] with N_2 shows that a calculation which yields a reasonable value for the quadrupole moment may not give the slope accurately. Since at this stage we want to calculate the rate constant using parameters the value of which cannot reasonably be disputed, we will reserve talking about the contribution of higher multipoles until later.

The probability of energy transfer per collision, P, due to dipole-dipole coupling is[4, 5]

$$P_{dd} = P(b = 0) + 1.5\ P(b = d) \qquad (32)$$

where P (b = 0) and P (b = d) are the values of P for impact parameters equal to zero and hard sphere diameter, respectively. Previous experience shows that P (b = 0) is about 10% of the total P. Since our calculation does not have this accuracy, we will neglect the first term

on the right hand side of Eq. (32). Following Ref. 4 we can write

$$P_{dd} \quad 4\pi^{-2} \frac{M}{kT} d^{-4} \left[\mu_{01}^{(1)} \mu_{10}^{(2)}\right]^2 x \sum_{\substack{j_i, j_i' \\ i=1,2}} \prod_{i=1,2} \left[\eta_{j_i}^{(i)} C^2(j_i 1 j_i'; 00)\right] I_2'(x) \tag{33}$$

where M is the reduced mass of the collision pair, $\mu_{01}^{(1)}$ and $\mu_{10}^{(2)}$ are the transition moment for the ν_3 of CO_2 (molecule 1) and CO (molecule 2), respectively. The absolute square for the transition dipole moments was taken[8] to be 1.0×10^{-37} and 1.1×10^{-38} $(esu\text{-}cm)^2$ for CO_2 and CO, respectively. The term d is the hard sphere diameter, $d = 3.82 \times 10^{-8}$ cm,[21] $\eta_{j_i}^{(i)}$ is the probability of finding molecule i in the level j_i, $C(j_i 1 j_i; 00)$ are the reduced Clebsch-Gordon coefficients and $I_2'(x)$ is the Fourier transform of the dipole-dipole potential given by

$$I_2'(x) = (0.3333 + 0.2618\, x^2)\, f_1(x) + 0.3334\, x\, f_{11}(x) + 0.1964\, y\, f_0'(x), \tag{34}$$

$x = 2\omega d\left(\frac{M}{2kT}\right)^{1/2}$, $f_n(x) = \int_0^\infty u^n e^{-[x/u + u^2]}\, du$ and $f_0'(x) = -\frac{d}{dx} f_0(x)$.

Figure 8 shows a plot of P_{dd} as a function of T^oK. The rate constant is strongly dependent upon temperature and, in contrast to the cases previously investigated, increases with temperature. The reason for this is as follows: In the theory of energy transfer using long range interactions, certain rotation selection rates are observed. For example, dipole-dipole interaction leads to $\Delta j_1 = \Delta j_2 \pm 1$ rotational selection rates. Since the energy transfer probabilities are large if $\alpha \tau < 2$, where α is the absolute value of the energy that is transferred from internal degrees for freedom's

translation (radians sec^{-1}) and τ is the time duration of the collisions, those collisions which absorb most of the energy mismatch in rotations are strongly preferred. Since the energy mismatch that can be absorbed into rotations is proportional to j, and the higher rotational levels are more populated at higher temperatures, the cross-section increases with temperature, the P_{dd} vs T curve will begin to level off at a temperature T_1 such that $2 B_1 J_{m_1} + 2 B_2 J_{m_2} \approx \Delta E$, where J_{m_1} and J_{m_2} are the most probable values of the rotation quantum numbers at the temperature T_1 and ΔE is the energy mismatch. With further increase of temperature, P is expected to show a negative temperature dependence. Figure 8 actually shows P_{dd} for those rotational transitions for which $\Delta j_{CO_2} = \Delta j_{CO} = + 1$. The transitions $\Delta j_{CO_2} = - 1$ and $\Delta j_{CO} = + 1$ make a contribution to P_{dd} that is 20 times smaller. In the second order calculation, the virtual state may be an excited electronic state of one molecule (Debye induction interaction) and/or of both molecules (dispersion interaction). In Ref. 7, it was shown that the contribution to the rate constant by these interactions is about two orders of magnitude smaller than the reaction paths in which virtual states are excited vibrational levels of the ground electronic states. In addition, following Ref. 7, we will neglect those virtual states in which both the molecules are either vibrationally excited or have no vibrational excitation. Figure 9 shows three sets of Feynman diagrams which have to be added to obtain the cross-section for the energy transfer. The final rotational states in Fig. 9a differ from those in Figs. 9b and 9c and therefore the cross-sections obtained from 9a add to those obtained from diagrams 9b and 9c. On the other hand, 9b and 9c can connect the same initial and final states

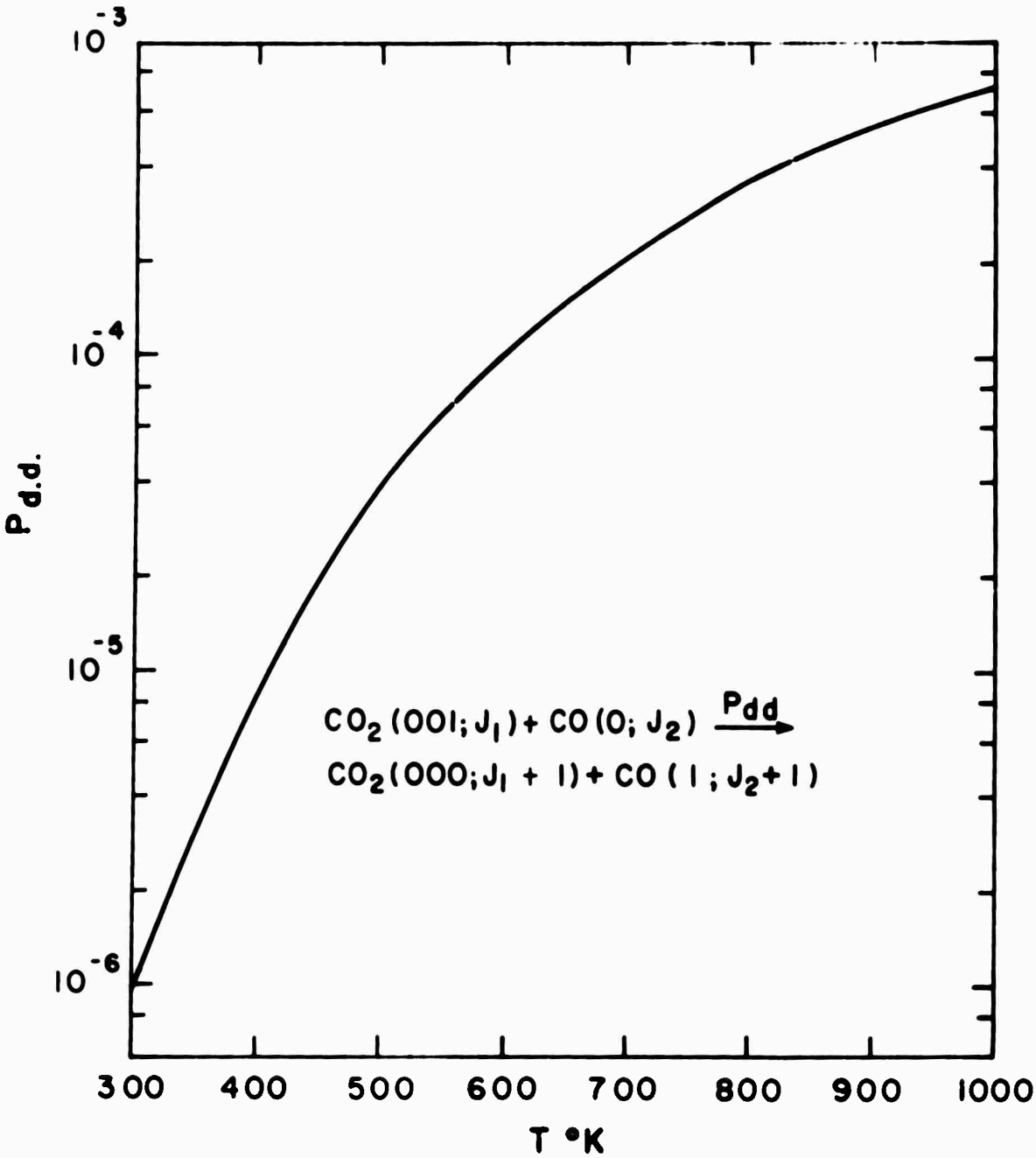

Fig. 8 CO_2, CO Dipole-dipole transition probability vs. temperature. For both CO_2 and CO $\Delta j = +1$.

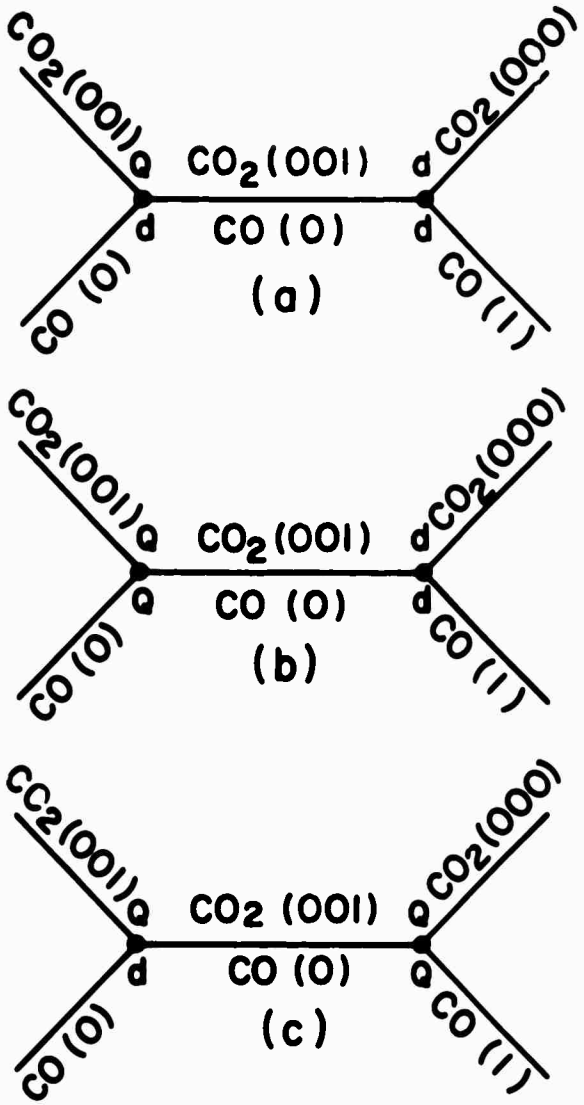

Fig. 9 CO_2/CO: Feynman diagrams. The multipole moments connecting initial states with a virtual state are shown on the left vertex, multipole moments connecting final states with a virtual state are shown on the right vertex (Q = quadrapole, d = dipole).

and primes denote their derivatives with respect to internuclear distance evaluated at the equilibrium internuclear distance. The calculations[10,11] show that Q and Q' have opposite signs. The calculations of CO dipole moment cited earlier give the sign (C^+O^-) opposite to that observed experimentally.[21] This is because of small dipole moment of CO. Minimization of energy gives a slightly distorted charge distribution yielding opposite signs. If we accept the result arrived at by calculation[10] that at large distance the sign of the dipole moment is C^+O^-, one is led to the conclusion that dipole moment and its derivative have opposite signs. In this case then, the interference between diagrams 9b and 9c is constructive. In calculating the contribution of diagram 9c to the rate constant we are again confronted with an uncertain value of Q'. Fortunately, the fact that CO has a small value of dipole moment is of help here. The relative contribution of Fig. 9b and 9c to the scattering amplitude is

$$\frac{\langle 0|\mu|1\rangle\langle 0|Q|0\rangle}{\langle 0|\mu|0\rangle\langle 1|Q|0\rangle} \text{ or } \frac{|\langle 0|Q|0\rangle|}{|\langle 1|Q|0\rangle|}, \text{ since } \frac{|\langle 0|\mu|1\rangle|}{|\langle 0|\mu|0\rangle|} \approx 1$$

For the scattering amplitude due to diagram 9c to be about 0.1 that of 9b $\langle 1|Q|0\rangle \approx 2.5 \times 10^{-27}$. This number is approximately 2.5 times the corresponding matrix element for N_2 and about 4 times larger than value obtained using molecular structure calculations.[10,11] Thus the inclusion of diagrams 9c is expected to give cross-sections which are at most about 10% larger than the one obtained by neglecting it. Since other assumptions in the calculation are greater source of error, we will neglect diagram 9c.

$$P = 5\hbar^{-2} \frac{M}{kT} d^{-14} C^2(2\,4\,6;00) \sum_{j_1, j_2} \prod_{i=1,2} \left(n_{j_i}^{(i)} \left(Q_1^{(i)} \; Q_2^{(i)} \right)^2 \right) S_6(x, 8) \times Z_1$$

(35)

$$(j_1, j_2, \Delta E).$$

where $(Q_1^{(i)'})^2$ is the absolute square of the dipole moment matrix element between the two vibrational levels, and $Q_2^{(i)}$ is the expectation value of the quadrupole moment of molecule (i). The expectation values of CO_2 and CO in the excited vibrational state are taken equal to their values in the ground vibrational level.

$$S_6(x, 8) = v^2 d^{+14} \left[\sum_{m=6}^{+6} \left| \left(\frac{4\pi}{13} \right)^{1/2} \int_{-\infty}^{+\infty} e^{i\omega t} \, Y_{6,m}^{*} \, R^{-8}(t) \, dt \right| \right]^2 \qquad (36)$$

where $x = \frac{\omega d}{v} = \omega d \left(\frac{M}{8k_T} \right)^{1/2}$, where $\omega = 2\pi c \tilde{\nu}$ is the absolute value of the energy transferred from internal degrees of freedom to translation. Z_1 depends upon the initial and final rotational levels and upon the energy mismatch in the following way:

(i) $j_1' = j_i + 3, \; i = 1, 2$

$$Z_1(j_1, j_2, \Delta E) = \left(\prod_{i=1,2} \frac{1.5(j_i+1)(j_i+2)(j_i+3)}{(2j_i+1)(2j_i+3)(2j_i+5)} \right) \left[\left[\sum_{i=1,2} 2B_i(2j_i+3) \right]^{-1} - \left[\Delta E - \sum_{i=1,2} 2B_i(j_i+1) \right]^{-1} \right]^2 \qquad (37)$$

(ii) $j_i' \quad j_1 + 1,\ j_2' \quad j_2 + 3$

$$Z_1 \quad \frac{0.4\, j_1 (j_1 + 1)(j_1 + 2)}{(2j_1 + 1)} \times \frac{1.5\,(j_2 + 1)(j_2 + 2)(j_2 + 3)}{(2j_2 + 1)(2j_2 + 3)(2j_2 + 5)} \times$$

$$\left[\frac{1}{(2j_1 + 3)} \left(\left(\frac{2j_1 + 5}{2j_1 - 1} \right)^{1/2} \left(2B_2 (2j_2 + 3) \right)^{-1} + \left(\frac{2j_1 - 1}{4(2j_1 + 5} \right)^{1/2} \times \right. \right.$$

$$\left(\sum_{i = 1, 2} 2B_i (2j_i + 3) \right)^{-1} \Bigg) - \frac{1}{(2j_1 + 1)} \left(\left(\frac{2j_1 - 1}{2j_1 + 5} \right)^{1/2} \times \right.$$

$$\left. \left. \left(\Delta E - \sum_{i = 1, 2} 2B_i (j_i + 1) \right)^{-1} + \left(\frac{2j_1 + 5}{4(2j_1 - 1} \right)^{1/2} \left(\Delta E + 2B_1 j_1 - 2B_2 (j_2 + 1) \right)^{-1} \right) \right]^2$$

$$\tilde{\nu} = \left| \Delta E - 2B_1 j_1 (j_1 + 1) - 6\, B_2 j_2 (j_2 + 2) \right| \tag{38}$$

Figure 10 shows a graph of P vs T for cases (i) and (ii). Figure 11 shows the P due to first order and second order process and their sum. Also shown are the experimental points obtained by Fig. 6 and Rapp's calculation for Eq. (30).

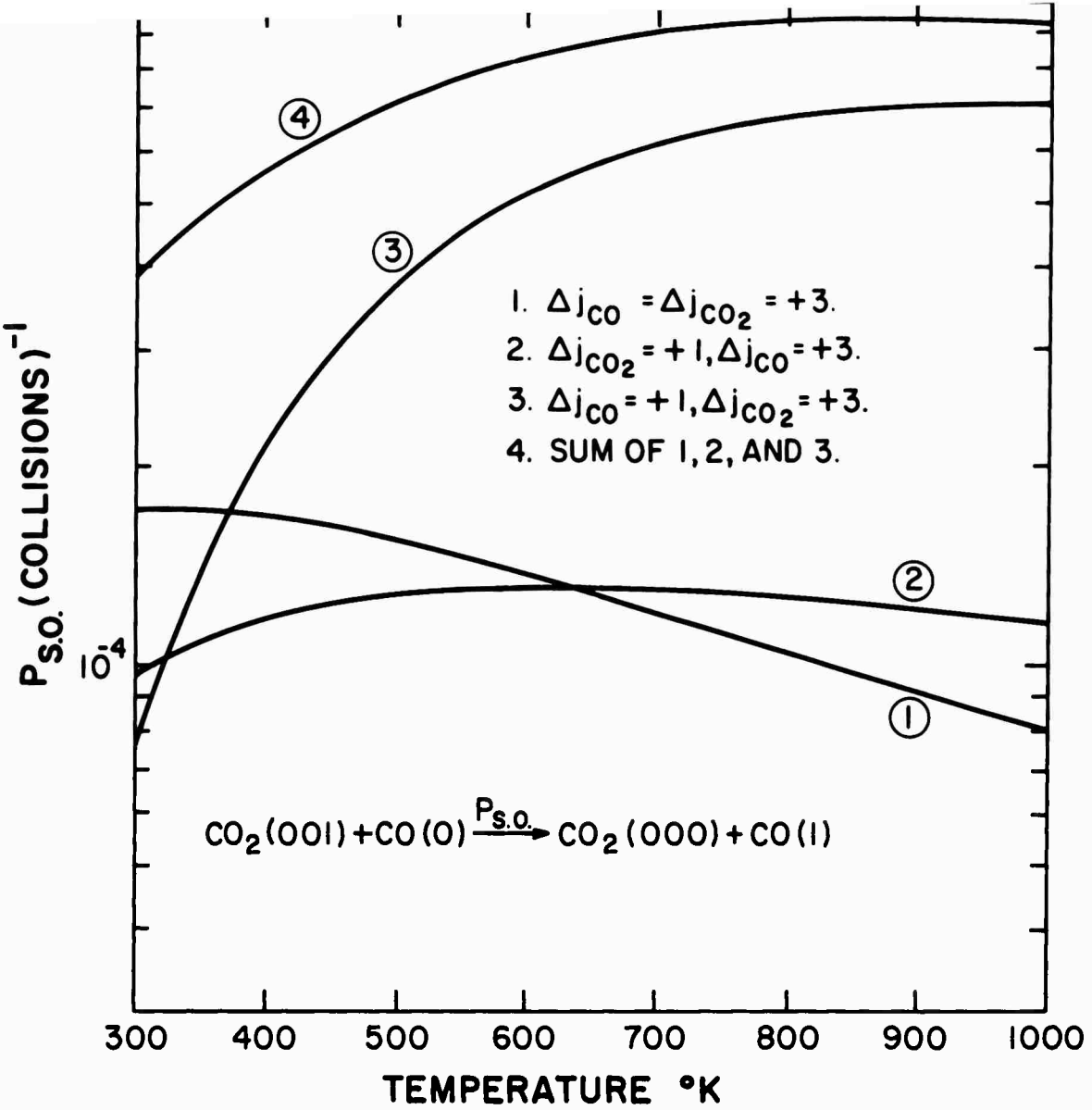

Fig. 10 CO_2/CO: Various second-order contributions to transition probability.

1. $\Delta j_{CO} = \Delta j_{CO_2} = +3.$
2. $\Delta j_{CO_2} = +1, \Delta j_{CO} = +3.$
3. $\Delta j_{CO} = +1, \Delta j_{CO_2} = +3.$
4. Sum of 1, 2, and 3.

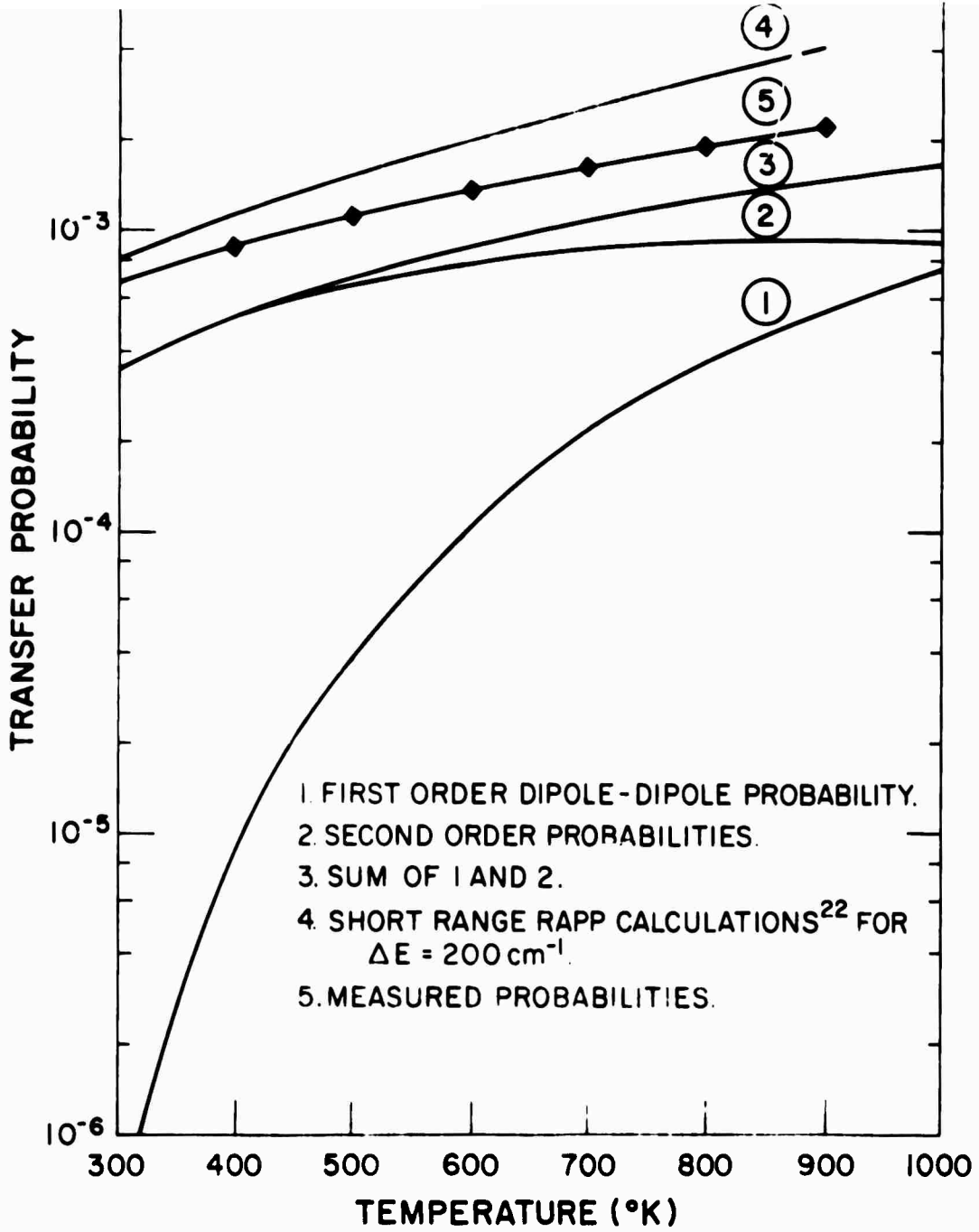

Fig. 11 CO_2, CO: Comparison of calculated with measured transition probabilities.

1. First order dipole-dipole probability.
2. Second order probabilities.
3. Sum of 1 and 2.
4. Short range Rapp calculations[19] for $\Delta E = 200\ cm^{-1}$.
5. Measured probabilities.

long range forces are within a factor of two off from the experimental data. In addition, both show approximately the same temperature dependence as the experimentally observed data. The long range forces calculation does not contain any adjustable parameters and its validity has been established by studying energy transfer from N_2O to CO_2(Eq. (31)). The short range force calculation used here is not directly applicable to CO_2-CO energy transfer process but was taken from a calculation of V-V energy transfer between two diatomic molecules with similar energy mismatch. Since short range calculations are almost always adjusted for the range parameter, it was not considered advisable to invest time in another short range force calculation. It is, however, quite conceivable that Rapp's calculation overestimates the short range contribution by a factor of 4. This, then, added to long range force cross-section would give a reasonable fit to the experimental data. This explanation, however, suffers from one draw back. Why should the contribution to the cross-section of the short range forces to CO_2-CO energy transfer process at 900^oK be about 10^{-4} and for CO_2-N_2 reaction less about 10^{-5}.

Another possibility is that short range forces in CO_2-CO energy transfer process do not play a role for the temperatures investigated here. Short range forces certainly do not play any role up to 1000^oK for CO_2-N_2 reaction. So this possibility is not obviously incorrect. The difference between the long range calculation and experimentally observed data may be due to the neglect of some of the Feyman diagrams, for example those which lead to $\Delta j_1 = \Delta j_2 = +1$. This possibility is currently being investigated.

ACKNOWLEDGMENT

The authors are greatful to Dr. D. Neumann for communicating the results of this calculation to us before publication.

REFERENCES

1. Rosser, W. A. Jr., Wood, A. D., and Gerry, E. T., J. Chem. Phys. 50, 4996 (1969).

2. Hocker, L. O., et al., Phys. Rev. Letters 17, 233 (1966).

3. Moore, C. B., et al., J. Chem. Phys. 46, 4322 (1967).

4. Sharma, R. D., and Brau, C. A., Phys. Rev. Letters 19, 1273 (1967); J. Chem. Phys. 50, 924 (1969).

5. Sharma, R. D., J. Chem. Phys. 50, 919 (1969); Phys. Rev. 177, 102 (1969).

6. Roach, J. F. and Smith, W. R., J. Chem. Phys. 50, 4114 (1969).

7. Sharma, R. D., Phys. Rev. A, 2, 173 (1970).

8. Penner, S. S., Quantitative Molecular Spectroscopy and Gas Emissivities (Addison-Wesley Publ. Co., Reading, Mass., 1959). p. 23.

9. Buckingham, A. D., Chemistry in Britain 1, 54 (1969).

10. Nesbet, R K., J. Chem. Phys. 40, 3619 (1964). For calculation of quadrupole moment at equilibrium internuclear distance; W. Huo, J. Chem. Phys. 43, 624 (1965), R. M. Stevens and M. Karplus, J. Chem. Phys. 49, 1094 (1968), D. B. Neumann and J. W. Moskowitz, J. Chem. Phys, 50, 2216 (1969).

11. Neumann, D. B., and Wasserman, Z., to be published.

12. Sokolnikoff, I. S., and Redheffer, R. M., "Mathematics of Physics and Modern Engineering," (McGraw-Hill Book Company, Inc., 1966), 2nd ed., p. 148.

13. Millikan, R. C., J. Chem. Phys. 38, 2855 (1963).

14. Benson, S. W., and Berend, G. C., J. Chem. Phys. 44, 470 (1966).

15. Calvert, J. C., and Amme, R. C., J. Chem. Phys. 45, 4710 (1966).

16. Thompson, S. L., J. Chem. Phys. 49, 3400 (1968).

17. Landau, L., and Teller, E., Z. Physik Sovjet Union 10, 34 (1936).

18. Schwartz, R. N., Slawsky, Z. I., and Herzfeld, K. F., J. Chem. Phys. 20, 1591 (1952). See also K. F. Herzfeld, ibid 47, 743 (1967).

19. Rapp, D., J. Chem. Phys. 43, 316 (1965).

20. Stephenson, J. C., Wood, R. E., and Moore, C. B., J. Chem. Phys. 48, 4790 (1968).

21. Rosenblum, B., Nethercot, A. H. Jr., and Townes, C. H., Phys. Rev. 109, 400 (1958).

22. Breshears, W. D., and Bird, P. F., J. Chem. Phys. 50, 333 (1969).

DOCUMENT CONTROL DATA - R&D

(Security classification of title, body of abstract and indexing annotation must be entered when the overall report is classified)

1 ORIGINATING ACTIVITY (Corporate author)
Avco Everett Research Laboratory
2385 Revere Beach Parkway
Everett, Massachusetts

2a REPORT SECURITY CLASSIFICATION
Unclassified

2b GROUP

3 REPORT TITLE

The Deactivation of Vibrationally Excited Carbon Dioxide (001) by Collisions with Carbon Monoxide

4 DESCRIPTIVE NOTES (Type of report and inclusive dates)
Research Report 349

5 AUTHOR(S) (Last name, first name, initial)

Rosser, W. A., Jr., Sharma, R. D. and Gerry, E. T.

6 REPORT DATE
September 1970

7a TOTAL NO OF PAGES
38

7b NO OF REFS
22

8a CONTRACT OR GRANT NO.
F29601-69-C-0060

b PROJECT NO
3326

c

d

9a ORIGINATOR'S REPORT NUMBER(S)
Research Report 349

9b OTHER REPORT NO(S) (Any other numbers that may be assigned this report)

10 AVAILABILITY/LIMITATION NOTICES

Distribution of this document is unlimited. This indicates document has been cleared for public release by competent authority.

11 SUPPLEMENTARY NOTES

12 SPONSORING MILITARY ACTIVITY Air Force Weapons Laboratory, Air Force Systems Command, United States Air Force, Kirtland Air Force Base, New Mexico and Advanced Research Projects Agency, ARPA Order No. 870

13 ABSTRACT

The rate constants associated with the deactivation of vibrationally excited CO_2* (001) by collisions with CO have been experimentally determined from 300 to 900 °K by a laser fluorescence method. These reactions involving CO were considered:

$$CO_2^*(001) + CO \underset{k_2}{\overset{k_1}{\rightleftharpoons}} CO_2 + CO^*(v=1)$$

$$CO_2^*(001) + CO \xrightarrow{k_{CO}} CO_2 + CO$$

$$CO^*(v=1) + CO_2 \xrightarrow{k_4} CO + CO_2.$$

Within experimental error the rate constant k_1 increases linearly with temperature T (°K) from a value of 5.7×10^3 torr^{-1} sec^{-1} at room temperature to a value of 11.2×10^3 torr^{-1} sec^{-1} at 900 °K. From 500 to 900 °K the rate constant k_{CO} (torr^{-1} sec^{-1}) varies with temperature as

$$\log_{10} k_{CO} = A - BT^{-1/3}$$

with A = 6.61 and B = 31.6. From 300 to 500 °K the measured values of k_{CO} are greater than those corresponding to the cited relation. The rate constant k_4 was found to be negligible compared to k_{CO}.

The probability per collision of vibrational energy transfer from CO_2* (001) to CO (v = 0) was computed by a theory involving long range forces. The calculated probabilities are in good agreement with the probabilities deduced from measurement of R_1, the transfer rate constant in the exothermic direction.

DD FORM 1 JAN 64 1473

UNCLASSIFIED

Security Classification

14 KEY WORDS	LINK A		LINK B		LINK C	
	ROLE	WT	ROLE	WT	ROLE	WT
1. Kinetics						
2. CO_2 Laser						
3. Upper laser level						
4. Fluorescence						
5. Vibration-vibration coupling						
6. CO						
7. Long range forces						

INSTRUCTIONS

1. ORIGINATING ACTIVITY: Enter the name and address of the contractor, subcontractor, grantee, Department of Defense activity or other organization (*corporate author*) issuing the report.

2a. REPORT SECURITY CLASSIFICATION: Enter the overall security classification of the report. Indicate whether "Restricted Data" is included. Marking is to be in accordance with appropriate security regulations.

2b. GROUP: Automatic downgrading is specified in DoD Directive 5200.10 and Armed Forces Industrial Manual. Enter the group number. Also, when applicable, show that optional markings have been used for Group 3 and Group 4 as authorized.

3. REPORT TITLE: Enter the complete report title in all capital letters. Titles in all cases should be unclassified. If a meaningful title cannot be selected without classification, show title classification in all capitals in parenthesis immediately following the title.

4. DESCRIPTIVE NOTES: If appropriate, enter the type of report, e.g., interim, progress, summary, annual, or final. Give the inclusive dates when a specific reporting period is covered.

5. AUTHOR(S): Enter the name(s) of author(s) as shown on or in the report. Enter last name, first name, middle initial. If military, show rank and branch of service. The name of the principal author is an absolute minimum requirement.

6. REPORT DATE: Enter the date of the report as day, month, year. If more than one date appears on the report, use date of publication.

7a. TOTAL NUMBER OF PAGES: The total page count should follow normal pagination procedures, i.e., enter the number of pages containing information.

7b. NUMBER OF REFERENCES: Enter the total number of references cited in the report.

8a. CONTRACT OR GRANT NUMBER: If appropriate, enter the applicable number of the contract or grant under which the report was written.

8b, 8c, & 8d. PROJECT NUMBER: Enter the appropriate military department identification, such as project number, subproject number, system numbers, task number, etc.

9a. ORIGINATOR'S REPORT NUMBER(S): Enter the official report number by which the document will be identified and controlled by the originating activity. This number must be unique to this report.

9b. OTHER REPORT NUMBER(S): If the report has been assigned any other report numbers (either by the originator or by the sponsor), also enter this number(s).

10. AVAILABILITY/LIMITATION NOTICES: Enter any limitations on further dissemination of the report, other than those imposed by security classification, using standard statements such as:

(1) "Qualified requesters may obtain copies of this report from DDC."

(2) "Foreign announcement and dissemination of this report by DDC is not authorized."

(3) "U. S. Government agencies may obtain copies of this report directly from DDC. Other qualified DDC users shall request through _____."

(4) "U. S. military agencies may obtain copies of this report directly from DDC. Other qualified users shall request through _____."

(5) "All distribution of this report is controlled. Qualified DDC users shall request through _____."

If the report has been furnished to the Office of Technical Services, Department of Commerce, for sale to the public, indicate this fact and enter the price, if known.

11. SUPPLEMENTARY NOTES: Use for additional explanatory notes.

12. SPONSORING MILITARY ACTIVITY: Enter the name of the departmental project office or laboratory sponsoring (*paying for*) the research and development. Include address.

13. ABSTRACT: Enter an abstract giving a brief and factual summary of the document indicative of the report, even though it may also appear elsewhere in the body of the technical report. If additional space is required, a continuation sheet shall be attached.

It is highly desirable that the abstract of classified reports be unclassified. Each paragraph of the abstract shall end with an indication of the military security classification of the information in the paragraph, represented as (*TS*) (*S*) (*C*) or (*U*).

There is no limitation on the length of the abstract. However, the suggested length is from 150 to 225 words.

14. KEY WORDS: Key words are technically meaningful terms or short phrases that characterize a report and may be used as index entries for cataloging the report. Key words must be selected so that no security classification is required. Identifiers, such as equipment model designation, trade name, military project code name, geographic location, may be used as key words but will be followed by an indication of technical context. The assignment of links, rules, and weights is optional.